

Direct molecular level characterization of different heterogeneous freezing modes on mica – Part 1

Ahmed Abdelmonem¹

¹Institute of Meteorology and Climate Research – Atmospheric Aerosol Research (IMKAAF),
Karlsruhe Institute of Technology (KIT), 76344 Eggenstein-Leopoldshafen, Germany

Correspondence to: Ahmed Abdelmonem (ahmed.abdelmonem@kit.edu)

Final Rebuttal

I. Point-to-point response to Referees

II. Revised manuscript with tracked changes

I. Point-to-point response to Referees

Point-to-point answers to the comments of Referee #1

The author would like to thank the referee for his time reading the manuscript and placing his comments.

RC: 1) The document is in a poor state of editing, with many grammatical errors that substantially distract from evaluating it.

AC: As the author is not a native English speaker the manuscript was revised by the “language service department” at the KIT before submission. Anyways, if the journal requires professional lingual editing by the journal itself or somewhere else, the author will certainly consider that.

RC: 2) The document contains false statements re: the origin of the SHG response. The system is probed off resonance, which means that all terms contributing to the response are purely real. Statements like "the SHG signal is originated from the the nonresonant OH stretching vibrations at the interface" are simply incorrect and reflect a fundamental misunderstanding of the signal generation process by the author. The signal is produced by all polarizable species within the SHG-active region. Unfortunately, the SHG active region is neither characterized nor defined in this work, making the signal interpretation at best appear as creative writing.

AC:

Indeed the statement "the SHG signal is originated from the nonresonant OH stretching vibrations at the interface", in page 2 line 19, is incorrect. However, it should be clear that this is not a “fundamental misunderstanding of the signal generation process by the author” but rather an oversight, wording failure, mixed with the definition of water stretching signal in SFG. This should have become clear to the reader when reaching to page 6 line 9 in the original manuscript when the author started discussing interpretations in terms of “electric dipolar contribution” as an origin of the signal. (This oversight has been corrected in the revised version, P. 2, L. 33-35)

The polarizable species at the surface are the water molecules and the surface OHs. The experiments were carried out in total internal reflection geometry with an incident angle of 15° from air to the prism side. The SHG-active region is limited by the penetration depth of the evanescent wave in the second medium (air, liquid water or ice). The calculated penetration depths are about 130 nm, 328 nm, and 253 nm for air, liquid water bulk, and ice bulk as contact media respectively (P. 6, L 11-12 in the revised manuscript).*

** Note: there was a typo in the corresponding incidence angles at interfaces in the original manuscript. This has been corrected in the revised version (P. 6, L. 1-3).*

RC: 3) The interference that is briefly alluded to in the final paragraph is not quantified, even though the changes in the SHG responses shown in the three figures are produced by said interference, in addition to changes in surface potential that occur during the experiments. The author is encouraged to read and understand the recent work on nonlinear optical interference in thin-layer systems by Massari (J. Phys. Chem. Lett., 2016, 7 (1), pp 62–68) and on the $\chi^{(2)}$ and $\chi^{(3)}$ phase interference by Wang, Geiger, and Eienthal (Nature Communications, 7, 13587, 2016).

AC: The referee speaks here about the “Two-Interface Problem” and refers to the work of Massari (*J. Phys. Chem. Lett.*, 2016, 7 (1), pp 62–68). Certainly, the author ignored this effect, and the mentioned paper is not relevant to the presented work, for the following reasons:

1. The mentioned work describes the interference between two resonant signals generated at the two interfaces (on two sides) of a well controlled thin-film prepared for an organic thin-film field-effect transistor. The two interfaces are well within the focal volume of the pump beams.
2. The signal interference occurs between two oppositely oriented groups, of the same type, at both sides of the thin-film
3. In contrast, ice (or liquid) -film growth on a surface is completely different. The growth depends mostly on the atmosphere saturation for a given temperature and pressure, and the thermal conductivity of the substrate material. When the air is supersaturated, the growth rate is very fast after nucleation and is very difficult to control.
4. In the presented work the second interface (ice-air or water-air) is not within the focal volume of the pump beam (please remember that the signal in the presented work was collected in TIR geometry) and the non-resonant signal is coming exclusively from the first interface (water-solid or ice-solid) due to the following: Under the thermodynamical conditions of the presented work, the ice (or water) layer thickness exceeds 1 μm within 1 sec which is far beyond the penetration depth of the evanescent field (see values above). The author would like to draw the attention of the referee to a related details on the growth velocity of a solidification front normal to the ice surface in the Supplementary Materials of the work of one of our KIT groups (Kiselev et al., 2016). These calculations were taken from numerous works of Libbrecht (Libbrecht, 2003; Libbrecht, 2005). For calculations of growth due to condensation, the reader is referred to the Aerosol Calculator Program (Excel) by Paul Baron which is based on equations from (Willeke and Baron, 1993; Hinds, 1999; Baron and KlausWilleke, 2001). These references have been cited in the revised version with the corresponding discussion (P. 6, L. 12-21)

The referee has also referred to the great paper on Phase-referenced nonlinear spectroscopy of the α -quartz/water interface by Wang, Geiger, and Eienthal (*Nature Communications*, 7, 13587, 2016) which shows that the absorptive (imaginary) and dispersive (real) terms of $\chi^{(2)}$ $\chi^{(3)}$ may mix. Again the author sees no significant relevance[†] to the presented work for the following reasons:

1. Regardless of the interesting role of the anisotropy of α -quartz to generate phase-referenced SHG signal, the mentioned paper discusses two extreme pHs (pH 3 and pH 11.5 which have 8.5 orders of magnitude hydrogen ion activity factor) and different ionic strengths. In contrast, in the presented work, neither the pH nor the ionic strength was changed. The author used deionized water with pH \sim 7.
2. The change of pH with temperature is very trivial for neutral water (e.g. from pH 7 at 25 °C to pH 7.47 at 0 °C). In addition, this does not mean that water becomes more alkaline at lower temperatures because in the case of pure water and according to the Le Châtelier's principle there are always the same concentration of hydrogen and hydroxide ions and hence, the water is still neutral (pH = pOH) even if its pH changes. The pH 7.47 at 0°C is simply the new reference of neutral water pH at 0 °C.

3. *Assuming that the surface potential has an influence on the background signal, this will not change even if the pH changes with temperature. It was found that the surface potential values of the muscovite basal plane (the surface under study) is pH independent in the range from pH 5.6 to 10 (Zhao et al., 2008).*

† Probably the author should have mentioned the chi(3) mechanism for interfacial potential-induced SHG which is an important factor in such experiments and has been originally established by the group of Eienthal (Zhao et al., 1993; Ong et al., 1992). This has been considered in the revised manuscript (P. 2, L. 37 – P. 3, L.4).

RC: 4) The work requires additional information on ice layer thickness, on the uniformity of the ice layers across the 2 mm laser spot, and it requires verification whether the SHG signal depends quadratically on input power. The polarization states of the SHG responses during the various stages of the experiments should also be determined.

AC: As mentioned above, the ice layer thickness exceeds the penetration depth of the evanescent field at the time when the signal was collected. The exact thickness cannot be determined in this setup, however it does not change the probed signal.

At the deposition, and also condensation, events the signal was not collected until it became stabilized and therefore, it was assumed that the ice layer is uniform at the surface covered by the laser spot. (Has been mentioned in the revised manuscript, P. 6, L. 21-23)

It was verified that $I(400) \propto I(800)^2$. (Has been mentioned in the revised manuscript, P. 3, L. 37-38)

As mentioned in page 3 line 26m, the SHG was collected S-polarized.

RC: 5) Connections of any results and/or discussion presented to the scientific motivation provided are not made except for two generic statements ("They provide novel molecular-level insight into different ice nucleation regimes..." and "Investigating the structuring of water molecules upon freezing next to solid surfaces is crucial to many scientific area...") which are broad and sweeping. In sum, this work is far too preliminary to be reconsidered. As such, this reviewer recommends rejection, with the hope that the author will write a new document that addresses the points made above in a new submission elsewhere.

AC: Certainly, the aim of the work was to demonstrate the worthwhile of investigating different ice nucleation processes and water structuring upon freezing on the molecular-level using SHG spectroscopy. This has been successfully demonstrated although conclusive description of ice nucleation on mica has not been obtained which is not expected at this stage. The manuscript is more like a "letter" or "short communication". However, ACP does not provide an individual category for particularly short papers because the process of peer review and publication in ACP is inherently efficient and rapid for all types of manuscripts without artificial length restrictions. A complementary study involving other techniques and sophisticated studies will follow this paper which is considered as a cornerstone for future studies. Probably a better title of the manuscript could be "Direct molecular level characterization of different heterogeneous freezing modes on mica – Part 1"

References:

- Baron, P. A. and Klaus Willeke: *Aerosol Measurement: Principles, Techniques, and Applications*, 2 ed., edited by: Sons, J., Wiley-Interscience, 2001.
- Hinds, W. C.: *Aerosol Technology: Properties, Behavior, and Measurement of Airborne Particles*, 2 ed., Wiley-Interscience, 1999.
- Kiselev, A., Bachmann, F., Pedevilla, P., Cox, S. J., Michaelides, A., Gerthsen, D., and Leisner, T.: Active sites in heterogeneous ice nucleation—the example of K-rich feldspars, *Science*, doi: 10.1126/science.aai8034, 2016.
- Libbrecht, K.: Growth rates of the principal facets of ice between -10°C and -40°C , *Journal of Crystal Growth*, 247, 530-540, doi: [https://doi.org/10.1016/S0022-0248\(02\)01996-6](https://doi.org/10.1016/S0022-0248(02)01996-6), 2003.
- Libbrecht, K. G.: The physics of snow crystals, *Rep. Prog. Phys*, 68, 855, doi: 10.1088/0034-4885/68/4/R03, 2005.
- Ong, S., Zhao, X., and Eisenthal, K. B.: Polarization of water molecules at a charged interface: second harmonic studies of the silica/water interface, *Chem. Phys. Lett.*, 191, 327-335, doi: 10.1016/0009-2614(92)85309-X, 1992.
- Willeke, K. and Baron, P.: *Aerosol Measurement: Principles, Techniques, and Applications*, edited by: Klaus Willeke, P. A. B., Van Nostrand Reinhold, 1993.
- Zhao, H., Bhattacharjee, S., Chow, R., Wallace, D., Masliyah, J. H., and Xu, Z.: Probing Surface Charge Potentials of Clay Basal Planes and Edges by Direct Force Measurements, *Langmuir*, 24, 12899-12910, doi: 10.1021/la802112h, 2008.
- Zhao, X., Ong, S., and Eisenthal, K. B.: Polarization of water molecules at a charged interface. Second harmonic studies of charged monolayers at the air/water interface, *Chem. Phys. Lett.*, 202, 513-520, doi: 10.1016/0009-2614(93)90041-X, 1993.

[Point-to-point answers to the comments of Referee #2](#)

The author would like to thank the referee for his time reading the manuscript and for the recommendations and suggestions.

RC: (1) The author stated that “the SHG signal is originated from the nonresonant OH stretching vibrations at the interface”. (Line 8 on page 4) This statement does not make sense. A nonresonant signal is by definition not to be associated with a particular vibrational mode.

AC: Indeed the statement "the SHG signal is originated from the nonresonant OH stretching vibrations at the interface", in page 2 line 19, is incorrect. The author has clarified this oversight failure in an earlier quick Author Comment on the discussion form because he expected that it may influence the general evaluation of the referees and the readers. This wording failure should however become clear to the reader when reaching to page 6 line 9 when the author started discussing interpretations in terms of "electric dipolar contribution" as an origin of the signal.

This has been corrected in the revised version, P. 2, L. 33-35.

RC: (2) Mica is birefringent. As the laser beam goes through the mica, its polarization may not be linear any more. “The advantage of using SM polarization combination is its dependence on only one non-vanishing nonlinear susceptibility tensor element (line 33 on page 3)” is likely not what has happened in the experiment.

AC: Before starting the measurements, the polarization of the water SHG signal was analyzed and found to have the expected maxima at S and P polarizations. (Has been mentioned in the revised version, P. 3, L. 35-37)

RC: (3) The index-matching gel of unknown chemical composition is a concern. While the gel helps to obtain the TIR condition, the gel/mica and gel/sapphire interfaces may produce SHG signal. The author may want to look into the freezing temperature of the gel too.

AC: The author would like to thank the referee for pointing out this missing information.

The IMG was obtained from Thorlabs (source and specifications has been mentioned in the revised version, P. 3, L. 38-39). The Flash point is > 220 °C. However, the freezing point is not specified by the manufacturer but tested in the lab. At least the gel was not frozen until -45 °C.

As already mentioned in the original manuscript, P. 3, L. 11 – 13, the influence of the temperature dependence of the optical properties of the index-matching gel, sapphire prism and mica on the SHG signal was studied before starting the series of measurements. There was no significant effect of the changes in the optical properties of these media on the detected signal within the range of freezing temperatures observed in the study. The Figure below (Fig. R2.1) shows the SHG at mica-N₂ gas interface in the range of freezing temperatures mentioned in the manuscript.

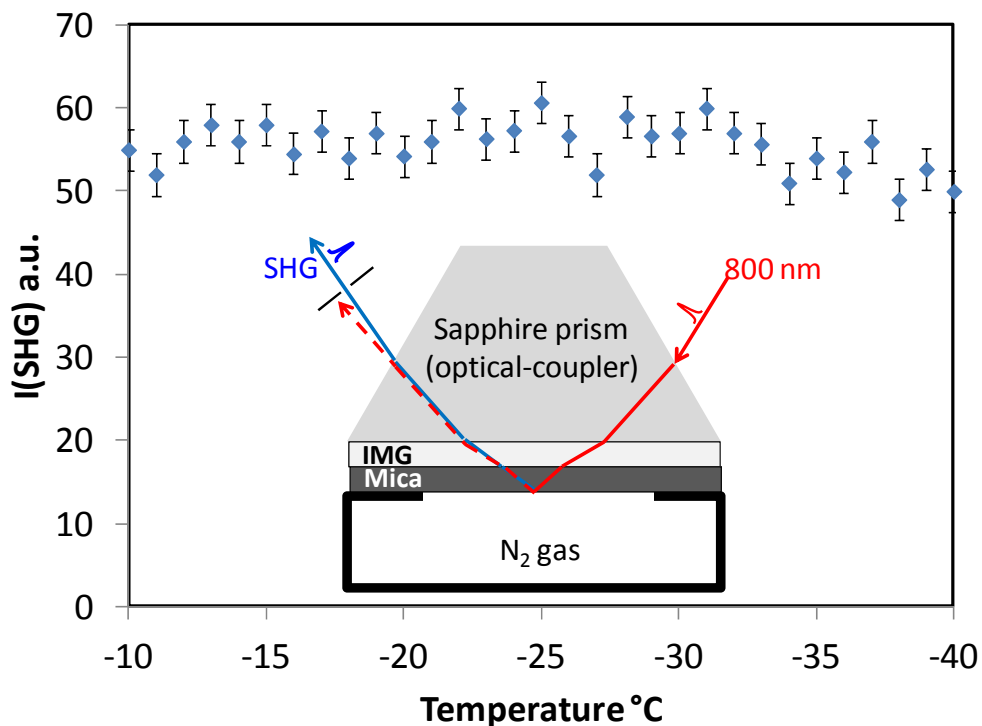


Figure R2.1: SHG at mica- N_2 gas interface in the range of freezing temperatures observed in the study. The cell, shown in Figure S2 in the original SI, was filled with ultrapure N_2 gas (99.9999 %).

Figure R2.1 and the corresponding text have been added to the SI of the revised manuscript.

RC: (4) Figure 1 and 2 should be real-time plots similar to Figure 3.

During the experiments, except for those of Figure 3, the signal was collected, averaged and stored as a function of the state of condensation, deposition, freezing, or formation of bulk. There was no need to record the data as a function of time. However, Fig. 3 is a special case because it was intended to report on the detected transient ice formed upon immersion freezing. Anyways, in the Figure below (Fig. R2.2), I show some screen shots of typical SHG signal and temperature changes in time, and show the points where the signal was collected and averaged.

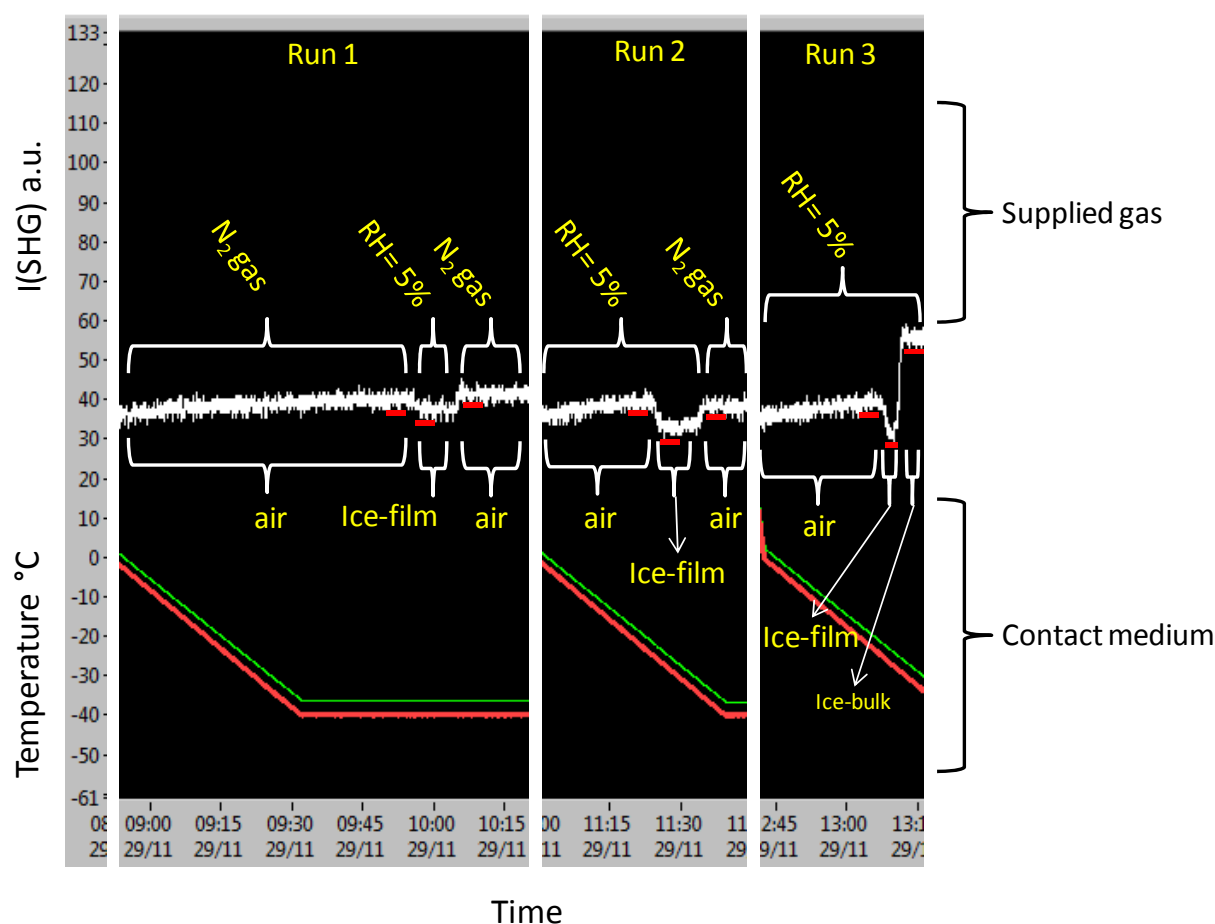


Figure R2.2: Screen shots of typical signal and temperature changes in time during arbitrary cooling processes. The white line shows raw SHG data. The short red dashes below the SHG data show the points where the signal was collected and averaged. The red and green lines show the temperatures of the sample bottom and sample top respectively.

Figure R2.2 shows three examples of three arbitrary experiments (Runs):

Run1: The cell was purged continuously with N₂ gas while cooling the sample down to -40. There is a small gradual change in the signal due to the changes in the temperature dependent optical constants. The cell was then purged with humid air which resulted in a formation of an ice-film by deposition. Finally, the cell was purged again with N₂ gas which resulted in sublimation of the ice film.

Run2: The cell was purged with humid air (RH=5%) while cooling the sample down until the formation of an ice film and then the cell was purged by N₂ gas which resulted in film sublimation.

Run3: The cell was purged with humid air (RH=5%) while cooling the sample down until the formation of an ice film. Purging the cell with humid air was continued until the formation of bulk ice.

All experiments of deposition freezing were done in a similar way as described above. Figures 1 and 2 in the manuscript show the averaged signal at each event and the error bars on the figures show the fluctuation in the data points among all repeated experiments.

This part has been included in the revised SI of the manuscript.

RC: (5) Terms such as “liquid (film)”, “liquid (bulk)”, “transient ice”, “stable ice” used in Figure 2 should be experimentally defined.

This is a very good point and was missing in the original manuscript. The border between a film at the solid-air interface and a bulk (ice or water) was defined experimentally by the point where the intensity of a TIR reflected light from the solid-air interface drops due to the violation of TIR condition when the refractive index of the contact medium changes drastically from that of air ($n_a=1$) to one of those of water or ice ($n_{w \text{ or } i} > 1.3$). Whether the contact medium is ice or liquid, this was defined by the strong light scattering, observed at a CCD camera placed close to the detection path (Fig. R2.3), when the ice is formed. This camera was missing in Fig. S1 in the SI of the original manuscript and will be added in the revised version (now Fig. 1 in the revised manuscript).

After immersion freezing, there was a rapid increase in the signal and then slow decrease. The maximum after the rapid increase was defined as the “transient ice” data point. After reaching a maximum, the signal was decreasing with time until stabilized after certain time. This stabilized signal was defined as the “stable ice” data point

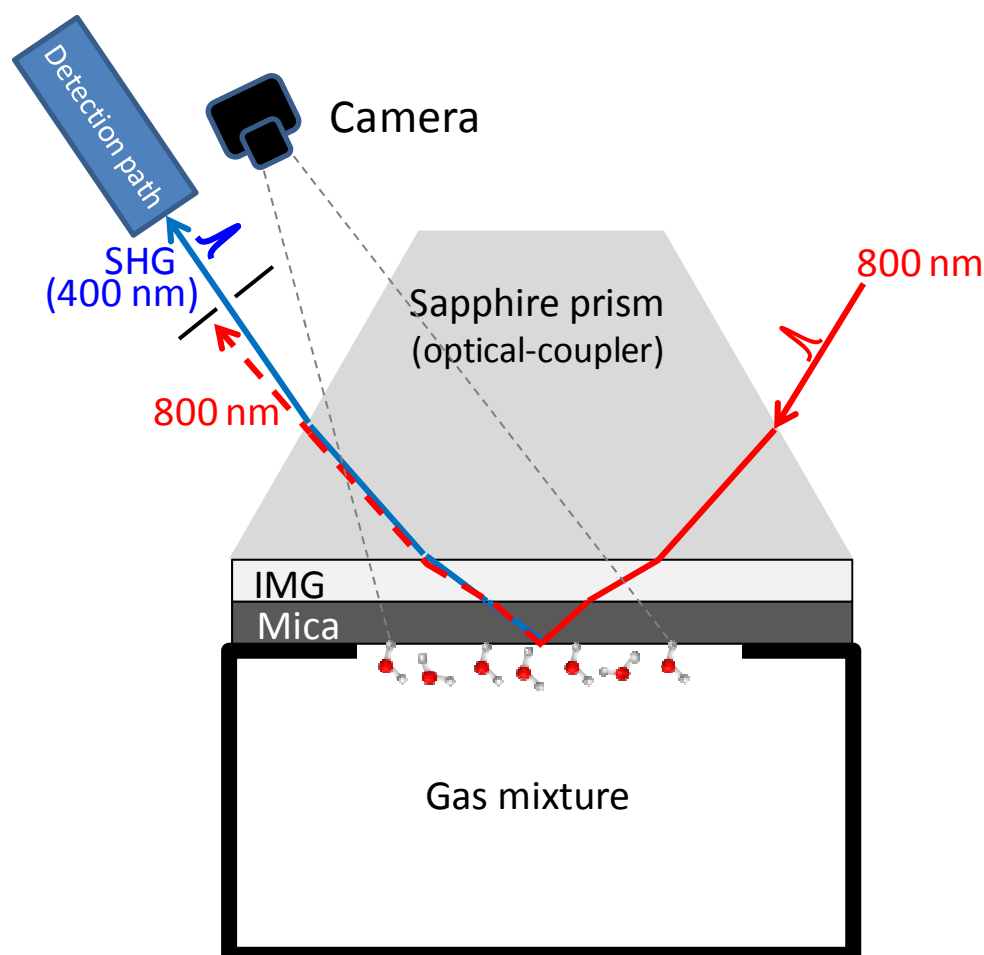


Figure R3.3: The same as Fig. S1 but with including the CCD camera (Guppy F-036 Allied Vision Technology with LINOS Macro-CCD Lens 0.14x (1:7) f4)

The text in the revised manuscript has been changed correspondingly, (P. 5, L. 3-11).

RC: (6) The cooling rate dependence should be investigated.

The results and conclusion were limited to the given cooling rate. Investigation of the influence of cooling rate was not planned in this work. However, the cooling rate dependence was tested in immersion freezing on sapphire surface using SFG in different study (under publication). It was found that the different cooling rates do not change the spectroscopic results.

RC: (7) One fundamental issue of SHG is that SHG intensity can be difficult to interpret. For example, why is there a ~80% SHG drop from the “air” to the “bulk liquid” in Figure 2? What does the SHG measure?

This is indeed a good question. The SHG signal is mainly produced by all polarizable species within the SHG-active region as long as the inversion symmetry is broken. The polarizable species at the surface are the water molecules and the surface OHs. The contribution of water molecules are limited by the penetration depth. The experiments were carried out in total internal reflection geometry with an incident angle of 15° from air to the prism side. The SHG-active region is limited by the penetration depth of the evanescent wave in the second medium (air, liquid water or ice). The calculated penetration depths are about 130 nm, 328 nm, and 253 nm for air, liquid water bulk, and ice bulk as contact media respectively. (This part has been added to the revised version, P. 6, L. 8-12).*

** Note: there was a typo in the corresponding incidence angles at the interfaces in the original manuscript. This has been corrected in the revised version, (P. 6, L. 1-3).*

The 80% drop of the signal was explained in the final paragraph of page 6 in the original manuscript. The included interpretation (different phase interference part) was discussed with Prof. Mischa Bonn (Director of the Molecular Spectroscopy department in Max Plank Institute for Polymer research, Mainz, Germany). However, the author agrees with the referee that this part was not well explained in the manuscript. Here is a more detailed discussion:

“Since SHG response reflects the overall arrangements of the polar entities at the interface between two isotropic media (Fordyce et al., 2001; Goh et al., 1988; Luca et al., 1995a), signal intensity is expected to increase when a single (or few non-centrosymmetric) layer(s) of water or ice is(are) formed at the surface. It is clear from Figures 1 and 2, however, that SHG intensity decreases upon deposition freezing, condensation, and growth of liquid layers by diffusion. This can be explained by phase interference between two signals originating from two different interfacial groups of opposite dipole moments: surface-OH points out of the surface and water points to the surface. A cleaved mica surface exhibits a disordered hexagonal arrangement of Si- (partly Al-) doubly coordinated O atoms in the outermost layer (Ostendorf et al., 2008). As an aluminosilicate mineral, this surface may protonate immediately in contact with the ambient air (forming silanol and aluminol groups at the surface). In this case, the mica-dry air signal can mainly originates from the surface hydroxyl groups (dangling-OH) which are naturally pointing out from the surface. Since mica surface is inherently negatively charged, the interfacial water will point to the surface and thus have a phase opposite to that of the surface-OH groups, as was reported by Shen and co-workers (Zhang et al., 2008) on negatively charged surfaces. This well explains the ostensible decrease in the overall signal upon deposition and condensation. When the surface of mica is covered with bulk water of a pH (~ 7) relatively higher than the point-of-zero-charge (pzc) of the surface, it becomes totally deprotonated

(no free-OH). Under this condition the SHG signal comes exclusively from the interfacial water molecules between the surface and liquid-bulk. This defines a new reference of the signal generated at the new interface (liquid-solid rather than gas-solid). The increase of the signal afterwards indicates more structuring of either the interfacial water before freezing, like shown in (Abdelmonem et al., 2015) or the interfacial ice after freezing like shown here. It is worth to mention that, the presence of free surface hydroxyl groups on cleaved mica is poorly discussed in literature. Miranda et al. have indirectly referred to their (hydroxyl groups) existence in their work on mica-water vapor interface using SFG (Miranda et al., 1998). They used deuterated water (D_2O) in the SFG experiments to avoid confusion of the hydroxyl stretch modes in the spectrum from both water and mica. Maslova et al. have discussed it a bit explicit in their work on surface properties of cleaved mica and they assumed that hydroxyl groups of the basal plane are not reactive (Maslova et al., 2004). One in four Si in the tetrahedral layers of mica is randomly substituted for Al (Christenson and Thomson, 2016). The result is that the majority of the surface hydroxyl groups of a cleaved basal plane are silanol and therefore the surface deprotonation is mostly determined by silica. The pzc value of silica lies between its respective isoelectric points (pH 2-3, (Hartley et al., 1997; Iler, 1979; Scales et al., 1992)) and hence the silanols in silica (Si-OH) deprotonated totally in the presence of neutral water.”

The final paragraph in the manuscript has been changed correspondingly.

RC: (8) Some conclusions made in the manuscript are not well supported by the SHG data. For example, line 8 on page 4: “The coincidence of the SHG signals of the thin ice film formed in DF2 and DF3 indicates identical structuring of water on the surface in two-step deposition freezing regardless of the onset temperature.” SHG simply cannot provide the structural information of water. The same SHG intensity does not necessarily mean the same water structure.

SHG is electric dipole forbidden in the centrosymmetric bulk media and therefore SHG has been widely used as the spectroscopic probe for molecular orientation, structure, and spectroscopy of different interfaces (Richmond et al., 1988; Goh et al., 1988; Goh and Eisenthal, 1989; Zhao et al., 1993; Conboy et al., 1994; Luca et al., 1995b; Eisenthal, 1993; Eisenthal, 1996; Antoine et al., 1997; Fordyce et al., 2001; Zhang et al., 2005; Pham et al., 2017). The SHG response relates to the overall arrangements of the water (or more general interfacial) entities (Goh et al., 1988; Luca et al., 1995b; Fordyce et al., 2001). However, probably the sentence “... indicates identical structuring...” is overstated. This sentence has been tempered in the revised manuscript.

Finally the author would like to thank the referee again for his valuable comments which helped to improve the manuscript. The author would also like to emphasize that the aim of the work was to demonstrate the worthwhile of investigating different ice nucleation processes and water structuring upon freezing on the molecular-level using SHG spectroscopy. The manuscript is considered as a cornerstone of future complementary studies involving other surfaces, and other techniques to precisely investigate the layer thickness, the surface morphology effect, the cooling rates ...etc. Probably a better title of the manuscript could be “Direct molecular level characterization of different heterogeneous freezing modes on mica – Part 1”

References:

- Abdelmonem, A., Lützenkirchen, J., and Leisner, T.: Probing ice-nucleation processes on the molecular level using second harmonic generation spectroscopy, *Atmos. Meas. Tech.*, **8**, 3519-3526, doi: 10.5194/amt-8-3519-2015, 2015.
- Antoine, R., Bianchi, F., F. Brevet, P., and H. Girault, H.: Studies of water/alcohol and air/alcohol interfaces by second harmonic generation, *Journal of the Chemical Society, Faraday Transactions*, **93**, 3833-3838, doi: 10.1039/a703711b, 1997.
- Conboy, J., Daschbach, J., and Richmond, G.: Studies of Alkane/Water Interfaces by Total Internal Reflection Second Harmonic Generation, *The Journal of Physical Chemistry*, **98**, 9688-9692, doi: 10.1021/j100090a600, 1994.
- Eisenthal, K. B.: Liquid interfaces, *Accounts of Chemical Research*, **26**, 636-643, doi: 10.1021/ar00036a005, 1993.
- Eisenthal, K. B.: Liquid Interfaces Probed by Second-Harmonic and Sum-Frequency Spectroscopy, *Chem. Rev.*, **96**, 1343-1360, doi: 10.1021/cr9502211, 1996.
- Fordyce, A. J., Bullock, W. J., Timson, A. J., Haslam, S., Spencer-Smith, R. D., Alexander, A., and Frey, J. G.: The temperature dependence of surface second-harmonic generation from the air-water interface, *Mol. Phys.*, **99**, 677-687, doi: 10.1080/00268970010030022, 2001.
- Goh, M. C., Hicks, J. M., Kemnitz, K., Pinto, G. R., Heinz, T. F., Eisenthal, K. B., and Bhattacharyya, K.: Absolute orientation of water molecules at the neat water surface, *J. Phys. Chem.*, **92**, 5074-5075, doi: 10.1021/j100329a003, 1988.
- Goh, M. C. and Eisenthal, K. B.: The energetics of orientation at the liquid-vapor interface of water, *Chemical Physics Letters*, **157**, 101-104, doi: 10.1016/0009-2614(89)87216-1, 1989.
- Luca, A. A. T., Hebert, P., Brevet, P. F., and Girault, H. H.: Surface second-harmonic generation at air/solvent and solvent/solvent interfaces, *J. Chem. Soc. Faraday Trans.*, **91**, 1763-1768, doi: 10.1039/ft9959101763, 1995a.
- Luca, A. A. T., Hebert, P., Brevet, P. F., and Girault, H. H.: Surface second-harmonic generation at air/solvent and solvent/solvent interfaces, *Journal of the Chemical Society, Faraday Transactions*, **91**, 1763-1768, doi: 10.1039/ft9959101763, 1995b.
- Ostendorf, F., Schmitz, C., Hirth, S., Kühnle, A., Kolodziej, J. J., and Reichling, M.: How flat is an air-cleaved mica surface?, *Nanotechnology*, **19**, 305705, doi: 10.1088/0957-4484/19/30/305705, 2008.
- Pham, T. T., Jonchère, A., Dufrêche, J.-F., Brevet, P.-F., and Diat, O.: Analysis of the second harmonic generation signal from a liquid/air and liquid/liquid interface, *The Journal of Chemical Physics*, **146**, 144701, doi: 10.1063/1.4979879, 2017.
- Richmond, G. L., Robinson, J. M., and Shannon, V. L.: Second harmonic generation studies of interfacial structure and dynamics, *Prog. Surf. Sci.*, **28**, 1-70, doi: 10.1016/0079-6816(88)90005-6, 1988.
- Zhang, L., Tian, C., Waychunas, G. A., and Shen, Y. R.: Structures and Charging of α -Alumina (0001)/Water Interfaces Studied by Sum-Frequency Vibrational Spectroscopy, *J. Am. Chem. Soc.*, **130**, 7686-7694, doi: 10.1021/ja8011116, 2008.
- Zhang, W.-k., Zheng, D.-s., Xu, Y.-y., Bian, H.-t., Guo, Y., and Wang, H.-f.: Reconsideration of second-harmonic generation from isotropic liquid interface: Broken Kleinman symmetry of neat air/water interface from dipolar contribution, *The Journal of Chemical Physics*, **123**, 22471301 - 22471311, doi: 10.1063/1.2136875, 2005.
- Zhao, X., Ong, S., and Eisenthal, K. B.: Polarization of water molecules at a charged interface. Second harmonic studies of charged monolayers at the air/water interface, *Chemical Physics Letters*, **202**, 513-520, doi: 10.1016/0009-2614(93)90041-X, 1993.

[Point-to-point answers to the comments of SC #1](#)

SC1: I have read with interest the recent contribution of A. Abdelmonem to Atmospheric Chemistry and Physics Discussions. Second-harmonic generation (SHG) spectroscopy has the potential to be a powerful tool for investigating freezing at interfaces. However, there are a number of points regarding the mica surface and previous work with mica that should be taken into consideration in any revised manuscript. In particular, these points may lead the author to reconsider some of his interpretation of the results.

The author is grateful to Dr. Hugo K Christenson for his interest in the work and also for his valuable comments and constructive recommendations.

More information about air cleaved mica has been added to the manuscript, P. 2, L. 2-11.

SC: 1. The two-step nucleation process postulated by Campbell et al. in 2013 involved various organic liquids crystallising from vapour on mica surfaces, but only in surface features such as cleavage steps, cracks and pockets. A later study (Campbell et al., 2017)) has confirmed the two-step process for the organic liquids, and strongly suggested a two-step process for water and ice, although conclusive proof could not be obtained for water and ice.

AC: Indeed, the discussion on the two-step process by (Campbell et al., 2013) in page 2 line 6 requires these details about the work. The author would also like to thank Dr. Christenson for drawing the attention to the very recent work by Campbell et al. on the two-step process (Campbell et al., 2017). The mentioned details and the recent work have been considered in the revised manuscript, P. 2, L. 17-24.

SC: 2. The material used by Layton and Harris in their 1963 paper (the reference is incomplete) was not muscovite mica but synthetic fluorophlogopite, which is similar in structure but has the hydroxyl groups replaced by fluorine. Moreover, neither is a metal oxide as stated in the abstract, but they are both layered aluminosilicates.

AC: Thanks for this clarification. The difference between the two micas as well as the corrected citation has been included in the revised manuscript, P. 2, L. 13-16.

SC: 3. The basal (cleavage) plane of mica consists of distorted hexagons of oxygen atoms, and there are no Si or Al atoms in the outermost layer. Moreover, the hydroxyl groups are below the oxygen hexagons, so there are none available for hydrogen bonding to adsorbed water molecules. This is explained in a recent review (Christenson and Thomson, 2016) which gives numerous references to the original literature on the structure determination of muscovite mica by X-ray diffraction.

AC: Probably the sentence in the manuscript was not clear enough (has been revised). Indeed, a cleaved mica surface exhibits a distorted hexagons of oxygen atoms in the outermost layer (Ostendorf et al., 2008) which are doubly coordinated with Si/Al atoms. My hypothesis is as follow: As an aluminosilicate mineral, this surface may protonate immediately in contact with the ambient air (forming silanol and aluminol groups at the surface). In this case, the mica-dry air SHG signal can mainly originate from the surface hydroxyl groups (dangling-OH) which are naturally pointing out

from the surface. A strong SHG signal was detected from the mica-air interface at 110 °C and under purging of N₂ gas before starting the cooling. The bulk hydroxyl groups cannot contribute to this signal. To my knowledge, the presence of free surface hydroxyl groups on mica is poorly discussed in literature. I could find only two articles discussing hydroxyl groups on mica basal plane: 1) Miranda et al. have indirectly referred to their (hydroxyl groups) existence in their work on mica-water vapor interface using SFG (Miranda et al., 1998). They wrote: "Deuterated water (D₂O) was used in the SFG experiments to avoid confusion of the hydroxyl stretch modes in the spectrum from both water and mica". This should mean that they observed a signal from those species (surface OH) in the OH vibrational region and, for this reason, they moved to the OD vibrational region. 2) Maslova et al. have discussed it a bit explicit in their work on surface properties of cleaved mica and they assumed that hydroxyl groups of the basal plane are not reactive (Maslova et al., 2004).

Since one in four Si in the tetrahedral layers is randomly substituted for Al (Christenson and Thomson, 2016), the majority of the surface hydroxyl groups of a cleaved basal plane are silanol and therefore the surface deprotonation is mostly determined by silica. The point-of-zero-charge (pzc) value of silica lies between its respective isoelectric points (pH 2-3, (Hartley et al., 1997; Iler, 1979; Scales et al., 1992)) and hence the silanols in silica (Si-OH) deprotonated totally in the presence of neutral water.

SC: 4. The simulation by Odelius et al. (1997) suggested that the mica surface is covered by a network of hydrogen bonds between water molecules only, with no free water hydroxyls. However, these results have been called into doubt by more recent simulations (Wang et al., 2005; Malani and Ayappa, 2009), and in a density-functional study that found no evidence of 2D-ice on mica, but that the properties of water on the surface are dominated by hydration of potassium ions (Feibelman 2013).

AC: The author is thankful for this clarification and probably referring to this work in the last paragraph was not correct (Has been removed in the revised version).

SC: 5. The study of air-cleaved mica and water vapour (as is the case here for the measurements in water vapour) is complicated by the fact that the surface potassium ions are free to diffuse along the surface (as potassium carbonate), which may even result in the formation of crystallites on the surface in dry conditions. This was first shown by Christenson and Israelachvili in 1987, and was discussed in Balmer et al., 2008. The implications for studying mica in humid atmospheres was summarised in the 2016 review mentioned under point 3. Mica immersed in bulk water does not suffer from these problems, of course, as any potassium carbonate dissolves and the nature of the surface ions is determined by the pH and any residual electrolyte in the solution. The mobility of the potassium ions (as potassium carbonate) does not necessarily alter dramatically any measurement of average surface properties, as is the case with SHG, and at high humidities the potassium will be widely dispersed across the surface. However, the surface mobility of the potassium will necessarily decrease at lower temperatures, and there may be a dependence on the history of the mica surfaces. To summarise, it should be borne in mind that what is adsorbed to the mica surface is a thin film of aqueous potassium carbonate, the concentration of which varies with humidity and temperature, rather than pure water.

AC: As written in the original manuscript, P. 3, L. 23, the laser power was reduced to allow observable signal but not destroy the index-matching gel. The fluctuation in the signal due to reducing the laser power limited the sensitivity of the system to monitor minor changes which may arise from pre-adsorption of sub-monolayers or even few monolayers at temperatures higher than the dew point or freezing point (P. 3, L. 41 – P. 4, L. 3 in the revised manuscript). The thickness of the water layer at the time of collecting the signal is expected to be in the order of 1 μm (has been explained in the revised version, P. 6, L. 12-21) which should allow the potassium to be widely dispersed across the surface. In addition, the sample was washed several times in the cell and kept in either dry N_2 gas or humid air. The humid air was obtained from continuously N_2 -purged MQ water as described in the SI. It is also expected, under these conditions, that the K^+ ions are totally replaced by H^+ ions. Studying monolayer film needs experimental arrangements which are not available in our Lab at this moment.

References:

- Campbell, J. M., Meldrum, F. C., and Christenson, H. K.: Characterization of Preferred Crystal Nucleation Sites on Mica Surfaces, *Cryst. Growth Des.*, 13, 1915-1925, doi: 10.1021/cg301715n, 2013.
- Campbell, J. M., Meldrum, F. C., and Christenson, H. K.: Observing the formation of ice and organic crystals in active sites, *Proceedings of the National Academy of Sciences*, 114, 810-815, doi: 10.1073/pnas.1617717114, 2017.
- Christenson, H. K. and Thomson, N. H.: The nature of the air-cleaved mica surface, *Surface Science Reports*, 71, 367-390, doi: <https://doi.org/10.1016/j.surfrep.2016.03.001>, 2016.
- Hartley, P. G., Larson, I., and Scales, P. J.: Electrokinetic and Direct Force Measurements between Silica and Mica Surfaces in Dilute Electrolyte Solutions, *Langmuir*, 13, 2207-2214, doi: 10.1021/la960997c, 1997.
- Iler, R. K.: *The Chemistry of Silica: Solubility, Polymerization, Colloid and Surface Properties and Biochemistry of Silica*, John Wiley and Sons, New York, 896 pp., 1979.
- Maslova, M. V., Gerasimova, L. G., and Forsling, W.: Surface Properties of Cleaved Mica, *Colloid Journal*, 66, 322-328, doi: 10.1023/B:COLL.0000030843.30563.c9, 2004.
- Miranda, P. B., Xu, L., Shen, Y. R., and Salmeron, M.: Icelike Water Monolayer Adsorbed on Mica at Room Temperature, *Physical Review Letters*, 81, 5876-5879, doi: 10.1103/PhysRevLett.81.5876, 1998.
- Ostendorf, F., Schmitz, C., Hirth, S., Kühnle, A., Kolodziej, J. J., and Reichling, M.: How flat is an air-cleaved mica surface?, *Nanotechnology*, 19, 305705, doi: 10.1088/0957-4484/19/30/305705, 2008.
- Scales, P. J., Grieser, F., Healy, T. W., White, L. R., and Chan, D. Y. C.: Electrokinetics of the silica-solution interface: a flat plate streaming potential study, *Langmuir*, 8, 965-974, doi: 10.1021/la00039a037, 1992.

II. Revised manuscript with tracked changes

Direct molecular level characterization of different heterogeneous freezing modes on mica – Part 1

Ahmed Abdelmonem¹

5 ¹Institute of Meteorology and Climate Research – Atmospheric Aerosol Research (IMKAAF), Karlsruhe Institute of Technology (KIT), 76344 Eggenstein-Leopoldshafen, Germany

Correspondence to: Ahmed Abdelmonem (ahmed.abdelmonem@kit.edu)

Abstract. The mechanisms behind heterogeneous ice nucleation are of fundamental importance to the prediction of the occurrence and properties of many cloud types, which influence climate and precipitation. Aerosol particles act as cloud condensation and freezing nuclei. The surface–water interaction of an ice nucleation particle plays a major, not well explored, role in its ice nucleation ability. This paper presents a real–time–molecular–level comparison of different freezing modes on the surface of an atmospherically relevant ~~metal–oxide~~mineral surface (mica) under varying supersaturation conditions using second harmonic generation spectroscopy. Two sub-deposition nucleation modes were identified (one- and two-stage freezing). The nonlinear signal at water-mica interface was found to drop upon the formation of a thin film on the surface regardless of 1) the formed phase (liquid or ice) and 2) the freezing path (one– or two–step), indicating similar molecular structuring. The results also revealed a transient phase of ice at water–mica interfaces during freezing, which has a lifetime of around one minute. Such information will have a significant impact on climate change, weather modification, and tracing of water in hydrosphere studies.

20 **1 Introduction**

Clouds influence the energy budget by scattering sunlight and absorbing heat radiation from the earth and are therefore considered the major player in the climate system. Formation of ice changes cloud dynamics and microphysics because of the release of latent heat and the Bergeron-Findeisen process, respectively (Pruppacher and Klett, 1997). Ice nucleation in the atmosphere can be triggered heterogeneously by aerosol particles, ice-nucleating particles (INP), or occurs homogeneously at about -38°C (Pruppacher and Klett, 1997). Cloud evolution depends not only on temperature and humidity, but also on the abundance and surface characteristics of atmospheric aerosols. Understanding the factors that influence ice formation within clouds is a major unsolved and pressing problem in our understanding of climate (Slater et al., 2016). Field and laboratory experiments on cloud formation started decades ago (see (Schaefer, 1949; DeMott et al., 2011; Hoose and Mohler, 2012) and references therein) and are ongoing. A wide variety of results and observations has been obtained in cloud microphysics, especially with respect to the ice nucleation ability of atmospheric aerosol particles and, hence, the mechanisms of cloud dynamics, precipitation formation, and interaction with incoming and outgoing radiation. Aerosol particles act as cloud condensation nuclei for liquid clouds, immersion or contact freezing nuclei for mixed-phase clouds, and heterogeneous deposition nuclei for ice (cirrus) clouds. Depending on whether water nucleates ice from the vapor or the supercooled liquid phase, ice nucleation is classified as deposition nucleation or immersion nucleation, respectively. Despite numerous investigations aimed at characterizing the effect of particle size and surface properties of the INP, there is a lack of information about the restructuring of water molecules on the surface of INPs around the heterogeneous freezing point.

In this paper, discrimination between different modes of freezing of water on an ice-nucleating surface using nonlinear optical spectroscopy is demonstrated. Mica, a widely spread layered clay mineral and one of the most prominent mineral

surfaces due to its atomic flatness and chemical inertness produced by perfect cleavage parallel to the 001 planes (Poppa and Elliot, 1971), was selected as a model surface in this study. However, the image of an inert and atomically smooth surface prepared by cleavage of muscovite mica in an ambient atmosphere is not quite correct (Christenson and Thomson, 2016). Surface analytical techniques found that the surface of muscovite mica cleaved in laboratory air, as the case in this work, contains a water-soluble compound, almost potassium carbonate crystallites, which may cover few tenths of a percent of the surface area (Christenson and Israelachvili, 1987). Nevertheless, definitive chemical analysis showing its presence is not yet available. However, the mobility of the potassium ions as potassium carbonate does not necessarily affect significantly any measurement of average surface properties as in the case of this work, and at high humidities the potassium will be widely dispersed across the surface. The readers which are interested in more details on the nature of the mica surface in general and air-cleaved mica surface in particular are referred to the review paper of Christenson, H. K. and Thomson, 2016 and papers cited therein.

Mica, as natural particles, is believed to be among the most effective ice nucleating minerals in the deposition mode (Eastwood et al., 2008; Mason and Maybank, 1958). An early study, using a projection microscope, of deposition nucleation of ice on freshly cleaved synthetic fluorophlogopite mica, which is similar in structure to muscovite but has the hydroxyl groups replaced by fluorine, using a projection microscope, revealed that there is no growth of ice until saturation with respect to water is reached (Layton and Harris, 1963). The authors concluded that at temperatures above $-40\text{ }^{\circ}\text{C}$, the growth of ice on mica should be a two-step process: A nucleus forms as water and then freezes. Experimental evidence of two-step nucleation was also provided by (Campbell et al., 2013) using an optical microscope. With the help of a scanning optical microscope, they showed that the nucleation, of various organic liquids crystallising from vapour on mica surfaces, favored specific nucleation sites with surface features such as cleavage steps, cracks and pockets. However, they suggested that a supercooled liquid phase forms first and then freezes after it has grown to a size which thermodynamically favors the solid phase. These assumptions were based merely on thermodynamic observations (temperature and vapor supersaturation). A later study by the same group, has confirmed the role of the surface features and the two-step process for the organic liquids, and strongly suggested a two-step process for water and ice (Campbell et al., 2017). Recent MD simulations of deposition freezing revealed that water first deposits in the form of liquid clusters and then crystallizes isothermally from there (Lupi et al., 2014). So far, there has been no direct experimental evidence of two-step freezing based on probing the molecular structuring of water molecules next to the surface.

In this work, second-harmonic generation (SHG) in total internal reflection (TIR) geometry was used to probe the change in the degree of ordering of water on the surface of mica. SHG is a powerful and simple, compared to sum-frequency generation (SFG), surface-sensitive spectroscopic tool for studying molecules near surfaces and at interfaces (Shen, 1989b; Shen, 1989a). The amplitude and polarization of the generated field, as a function of the polarization of the incident fields, carry information on the abundance and structure of the interfacial molecules between two isotropic media (Jang et al., 2013; Rao et al., 2003; Zhuang et al., 1999). More details on SHG and SFG can be found in the experimental section and in SI. In the system described here, the SHG signal is originated from the ~~the~~-nonresonant ~~OH stretching vibrations at the interface~~ electric dipolar contribution of the interfacial molecules. The signal response relates to the overall arrangements of the interfacial entities (Fordyce et al., 2001; Goh et al., 1988; Luca et al., 1995) and propotional to the incident field and the second-order nonlinear susceptibility $\chi^{(2)}$ of the interface. When the interface is charged the static electric field due to the charge can induce a third-order nonlinear polarization due to the contribution of the third-order nonlinear susceptibility $\chi^{(3)}$ of the solution (Ong et al., 1992; Zhao et al., 1993). In this work, the contribution of $\chi^{(3)}$ to the total SHG signal has been ignored because there was no significant change in the interface charge with temperature. The change of pH with temperature is very trivial for neutral water (e.g. from pH 7 at $25\text{ }^{\circ}\text{C}$ to pH 7.47 at $0\text{ }^{\circ}\text{C}$). In addition, this change does not mean that water becomes more alkaline at lower temperatures because in the case of pure water and according to the Le Châtelier's principle there are always the same concentration of hydrogen and hydroxide ions and hence, the water is still

neutral (pH = pOH) even if its pH changes. The pH 7.47 at 0°C is simply the new reference of neutral water pH at 0 °C. In addition, assuming that the surface potential has an influence on the background signal, this will not change even if the pH changes with temperature because the surface potential values of the muscovite basal plane (the surface under study) is pH independent in the range from pH 5.6 to 10 (Zhao et al., 2008) More details of SHG and SFG can be found in SI.

5 The results provide new insight into heterogeneous freezing processes and show the suitability of the method for studying current issues relating to ice nucleation, which will contribute to its rapid development in the next years. Initially, I found that the SHG signal drops upon the formation of a thin film regardless of whether the freezing path consists of one- or two-steps and the initially formed phase, liquid or ice, indicating a similar molecular structuring. In addition, I observed a transient SHG signal after immersion freezing.

10 The hygroscopicity of mica is expected to play a ~~role~~ in the described processes. The hygroscopicity and Langmuir isotherm studies on mica are available in literature but only at room temperature where the sample and environment are at equilibrium (Balmer et al., 2008; Beaglehole et al., 1991; Hu et al., 1995). Such studies at supercooled surfaces are worth to do and could be a topic of future work. An AFM study at 21 °C showed no water absorbed on the surface of mica at RH = 18 % (Hu et al., 1995). The first uniform water phase, of large two-dimensional islands with geometrical shapes in epitaxial
15 relation with the underlying mica lattice, was observed at RH = 28 %. The growth of this water phase is completed when the humidity reaches 40 to RH = 50 %. In my experiments on mica it is not possible to detect sub-monolayers, at least at this stage, due to technical reasons mentioned later. In the presented work, only clear steps in the signal were considered.

2 Experimental

2.1 Materials and setup

20 All experiments were carried out using MilliQ water (18.2 MΩ·cm). The total organic content in this water is below 4 ppb. Mica samples were obtained from Plano GmbH, Germany. The mica samples were freshly cleaved parallel to the 001 plane in air right before use. The freshly cleaved mica exhibits a wetting surface (on which water was spreading visually). The SHG experiments were conducted using a femtosecond laser system (Solstice, Spectra Physics) with a fundamental beam of 800 nm wavelength, 3.5 mJ pulse energy, ~80 fs pulse width, 1 kHz repetition rate, and a beam diameter of ~2 mm at the
25 interface. The supercooled SHG setup and the measuring cell ~~were~~ are similar to those described in previous publications (Abdelmonem et al., 2015; Abdelmonem et al., 2017). Compared to the setup described in (Abdelmonem et al., 2015), a single fundamental beam incident on the interface was used, Fig. 1, and the SM (S-polarized SHG / 45°-polarized incident) polarization combination was measured. Figure 1 shows the sample and beam geometry. The polarization direction of the incident beam was controlled by a half-wave plate followed by a cube polarizer. The generated signal was collected using a
30 photomultiplier tube (PMT) placed downstream of an optical system including band pass filters for 400 nm and a polarization analyzer. Briefly, in the SHG experiments a sapphire prism ~~is~~ was used as an optical coupler to the surface of a thin mica substrate, the basal plane of which ~~is~~ was exposed to liquid water or water vapor. The fundamental beam had an incident angle of 15° with the surface normal of the outer side of the prism. Under this geometry, the reflected fundamental (800 nm) and generated SHG (400 nm) beams co-propagate to the sapphire-air interface at the other side of the prism at
35 which both beams are refracted at two different angles. Only the SHG signal was allowed to reach the detection path. Before starting the measurements, the polarization of the SHG signal generated from water at the surface was analyzed and found to have the expected maxima at S and P polarizations corresponding to an incident 45°-polarized light. The signal was quadratically dependent on the input power. To study mica in TIR geometry, an index matching gel (IMG) from Thorlabs (G608N3, RI~1.45186 at 800nm) was
40 is used to fix the mica sample on the hypotenuse of the sapphire prism. The freezing point was not specified by the manufacturer but tested in the lab. At least the gel was not frozen until -45 °C. A detailed description of sample geometry and the selection of the IMG was published in (Abdelmonem et al., 2015). Less than 15% of

the laser output power was coupled to the setup to not destroy the IMG. The fluctuation in the signal due to reducing the laser power limited the sensitivity of the system and it was not possible to monitor minor changes which may arise from pre-adsorption of sub-monolayers at temperatures higher than the dew point or freezing point.

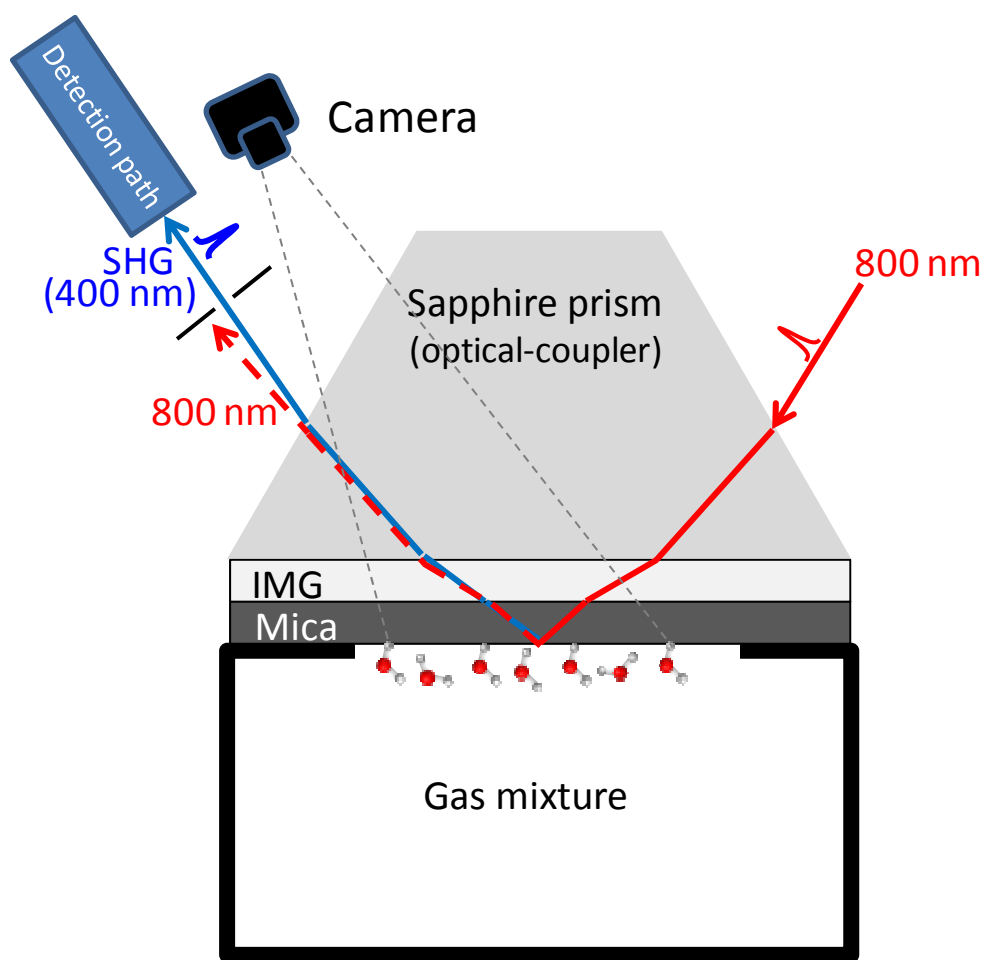


Figure 1: The sample and beams geometry. See text for details

A homemade temperature-controlled environmental chamber, Fig. 2, was integrated into the setup to control the sample temperature. A commercially available cold-stage (Linkam model HFS-X350) was used after modifying the housing to accommodate the SHG setup. The sapphire prism was placed in a copper adaptor which was fixed on the silver block of the Linkam cold-stage. The substrate of interest was sealed to a circular opening of 8 mm in diameter in a teflon cell which was being purged with the sample gas during the experiments. The cold-stage can perform controlled heating and cooling ramps, applied to the silver block, at rates between 0.01 and 100 °C/min. Temperature stability of the cold-stage is better than 0.1 K. The temperatures of the air inside the cell and the sapphire prism top and bottom were measured using four-wire-Pt100 elements. The temperature of the probed spot on the surface was considered to be the average of the sample top and sample bottom temperatures. However, it should be emphasized that the exact onset condition of freezing is not the focus of this work, but rather the study of the qualitative behavior of water molecules during freezing on the different paths. During the experiments, the gas box was filled with N₂ gas to avoid condensation on the outer surfaces of the prism during cooling. The humid air pumped to the measuring cell was obtained by mixing dry gas and 100 % humid gas with different ratios at 21 °C using two mass flow controllers (Tylan 2900). The continuous flow of the gas (either dry or humid) during the experiment set the temperature inside the cell to 21 °C ± 0.5 °C. The corresponding fluctuation of the relative humidity was less than 0.2%. The corresponding fluctuation in the dew point, at RH = 5 ± 0.2 for instance, was ±0.5 °C. The gas mixing ratio versus RH was calibrated by setting a mixing ratio, cooling the sample and recording the condensation/freezing temperature at

which the reflectivity at an angle equals to the critical angle of TIR for air-mica interface starts to drop due to the violation of TIR condition. This temperature was used to define the corresponding RH using Arden Buck equation.

The same method was used to differentiate between liquid-film, liquid-bulk, transient ice, and stable ice in this work. The border between a film at the solid-air interface and a bulk at the solid-water (or -ice) was defined experimentally by the point where the intensity of a TIR reflected light from the solid-air interface drops due to the violation of TIR condition when the refractive index of the contact medium changes drastically from that of air ($n_a=1$) to one of those of water or ice ($n_{w \text{ or } i} \geq 1.3$). Whether the contact medium is liquid or ice, this was defined by the change in the light scattering, observed at a CCD camera (Guppy F-036 Allied Vision Technology with LINOS Macro-CCD Lens 0.14x (1:7) f4) placed close to the detection path, Fig. 1. After immersion freezing, there was a rapid increase in the signal and then slow decrease. The maximum after the rapid increase was defined as the “transient ice” data point. After reaching a maximum, the signal was decreased with time until stabilized after certain time. This stabilized signal was defined as the “stable ice” data point.

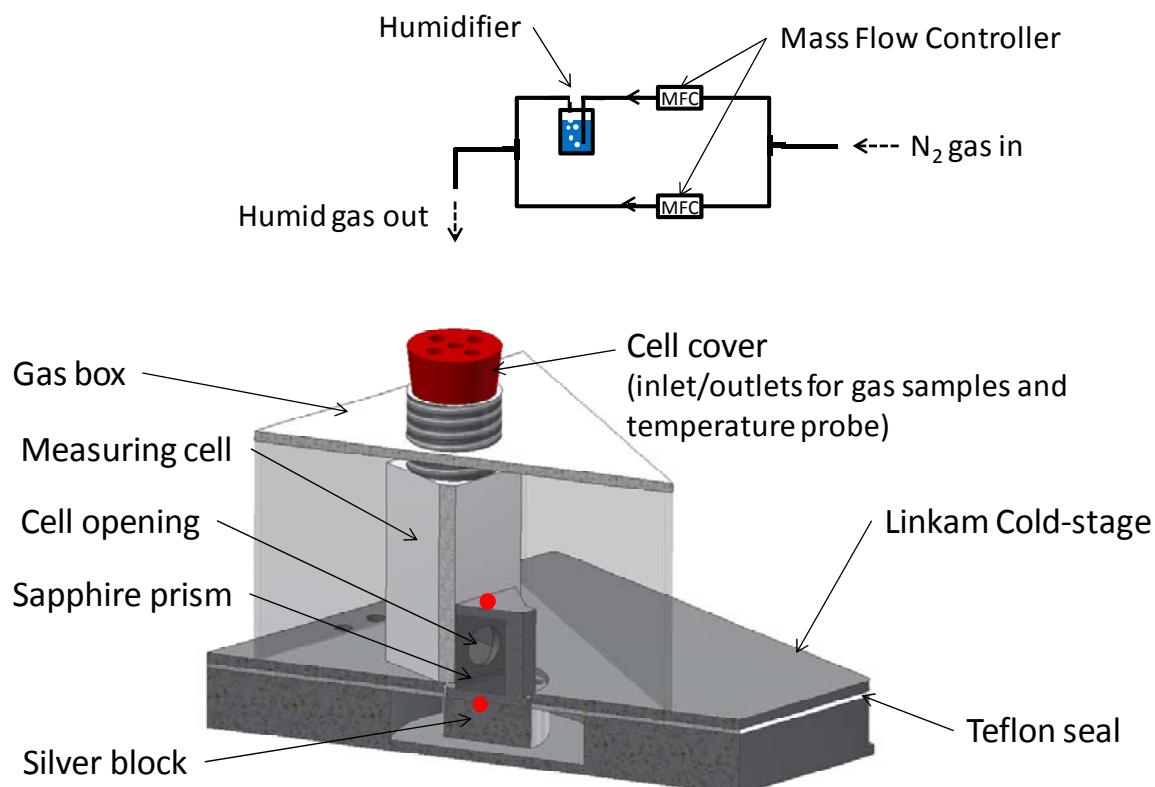


Figure 2: The temperature-controlled environmental chamber configuration, humidification and temperature sensors. The red dots are the position of the sample temperature sensors. There is a temperature sensor inside the measuring cell (not shown)

A ~~control~~Control software was developed to adhere to a predefined temperature profile and to measure the SHG signal and the temperature of the substrate. Temperature profiles were repeated several times for each sample to test reproducibility. In each run, the sample was heated to 110 °C while purging with N₂ gas (99.9999 %) to evaporate any residual water, then cooled down to 0 °C at a rate of 10 °C/min and then down to the heterogeneous freezing point at a rate of 1 °C/min. This cooling profile was the same for all runs to allow for logical comparison. An experiment with a mica-N₂ gas interface was carried out to ensure that the change in the refractive indices of the sapphire prism, IMG, and mica substrate with temperature had-have no significant effect on the resulting SHG signal in the range of freezing temperatures applied observed in this work, Figure S4 in SI. ~~During the freezing experiments, the substrate of interest was sealed to a circular opening of 8 mm in diameter in a teflon cell which was purged with a dry humid air mixture. The prism was inserted into a~~

5 tight housing of the cooling/heating stage. The temperatures of the sample top, sample bottom, and air mixture inside the cell were recorded using four wire Pt100 elements. This was not done to determine the exact onset conditions of freezing, but rather to study the qualitative behavior of water molecules during freezing on the different paths. The humidity of the gas mixture pumped to the measuring cell was adjusted by mixing N_2 gas with saturated water vapor at room temperature (21 °C). The mixing ratio was set using Tylan 2900 flow controllers.

10 The SHG experiments were conducted using a femtosecond laser system (Solstice, Spectra Physics) with a fundamental beam of 800 nm wavelength, 3.5 mJ pulse energy, ~80 fs pulse width, 1 kHz repetition rate, and a beam diameter of ~2 mm at the interface. Less than 15% of the laser output power was coupled to the setup to not destroy the IMG. The fluctuation in the signal due to reducing the laser power limited the sensitivity of the system to monitor minor changes which may arise from pre-adsorption of sub-monolayers at temperatures higher than the dew point or freezing point.

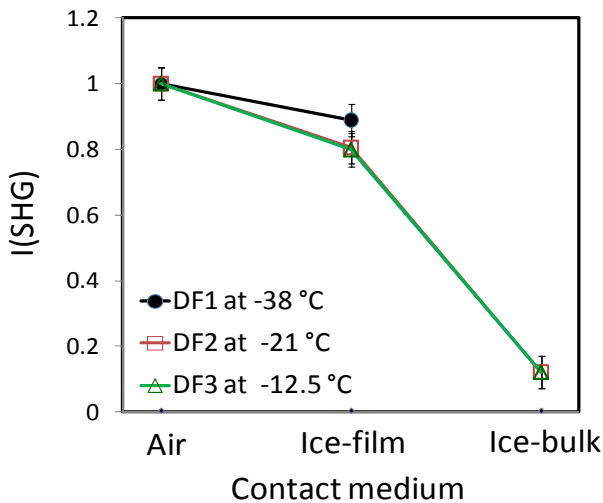
15 Compared to the setup described in (Abdelmonem et al., 2015), a single fundamental beam incident on the interface was used and the SM (S polarized SHG / 45° polarized incident) polarization combination was measured. The polarization direction of the incident beam was controlled by a half-wave plate followed by a cube polarizer. The generated signal was collected using a photomultiplier tube (PMT) placed downstream of an optical system including the appropriate filters and a polarization analyzer. As mentioned above, the incident angle from air of the fundamental beam was adjusted to 15° with respect to surface normal of the outer side of the sapphire prism. The corresponding incident angle on the mica-air or -water interface was ~ 51.663.4°, which is higher than the critical angles of TIR for mica-air (~34.139.7°) and mica-water (~50.259.2°) interfaces. This guaranteed a TIR condition regardless of any changes in the Fresnel factors caused by the change of refractive indices with changing temperature. The advantage of using SM polarization combination is its dependence on only one non-vanishing nonlinear susceptibility tensor element (χ_{yyz}), (Shen, 1989a; Zhuang et al., 1999), at any working angle which makes it a direct probe of the degree of order of the molecules at the interface.

20 The SHG signal is mainly produced by all polarizable species within the SHG-active region as long as the inversion symmetry is broken. The polarizable species at the surface of interest are the water molecules and the surface OHs. The contribution of water molecules are limited by the penetration depth inside the second medium (air, liquid water or ice). Under the optical geometry described above, the calculated penetration depths are about 130 nm, 328 nm, and 253 nm for air, liquid water bulk, and ice bulk as contact media respectively. Under the thermodynamical conditions of the presented work, the thickness of the ice (or water) layer should exceed 1 μ m within 1 sec after nucleation which is far beyond the penetration depth of the evanescent field. Therefore, although the exact thickness cannot be determined in this setup it does not affect the probed signal, by the Two-Interface Problem, because the second interface (ice-air or water-air) is not within the focal volume of the pump beam and the non-resonant signal is coming exclusively from the first interface (water-solid or ice-solid). For the ice layer thickness, the reader is referred to the calculations of the growth velocity of a solidification front normal to the ice surface provided in the Supplementary Materials of the recent work of Kiselev et al. (Kiselev et al., 2016). These calculations were taken from numerous works of Libbrecht (Libbrecht, 2003; Libbrecht, 2005). For calculations of growth due to condensation, the reader is referred to the Aerosol Calculator Program (Excel) by Paul Baron which is based on equations from (Willeke and Baron, 1993; Hinds, 1999; Baron and Willeke, 2001). The signal was not collected until it became stabilized and therefore, it was assumed that the ice layer after deposition was uniform at the surface covered by the laser spot.

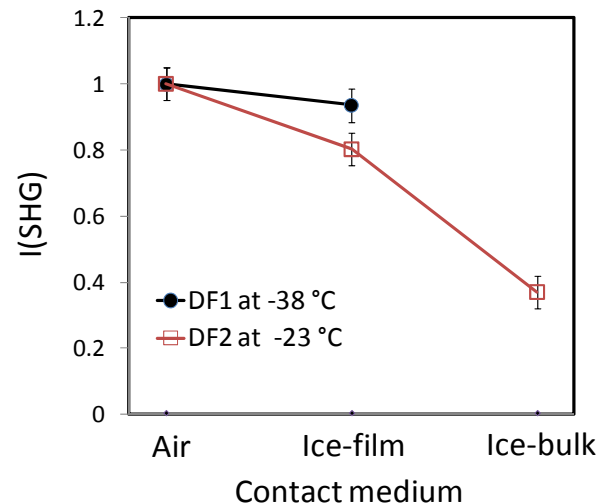
3 Results and discussion

40 The relative humidity (RH) of the purged gas was set to specific values in different runs to allow for different freezing modes on the surface of mica. Figure 4a-3a shows the change in normalized Fresnel factor-corrected (see SI for details) SHG

intensities under SM polarization combination for deposition freezing (DF) at $-38\text{ }^{\circ}\text{C}$ (black solid line and circles), $-21\text{ }^{\circ}\text{C}$ (red solid line and empty squares), and at $-12.5\text{ }^{\circ}\text{C}$ (green solid line and empty triangles) labeled by DF1, DF2, and DF3, respectively. In DF1, the cell was filled with N_2 gas and the sample was cooled down to a temperature, $-38\text{ }^{\circ}\text{C}$, far below the dew point at $\text{RH} = 5\%$ ($-21\text{ }^{\circ}\text{C}$). At $-38\text{ }^{\circ}\text{C}$, the cell was purged with humid air of $\text{RH} \sim 5\%$. An ice-film formed immediately on the surface, reflected by a drop in the SHG signal compared to that of air-mica interface. In DF2 and DF3, the cell was purged continuously with humid air of $\text{RH} = 5$ and 11% , respectively, and then cooled down until freezing and growth of ice were observed on the surface. Deposition freezing and the formation of an ice-film started at -21 and $-12.5\text{ }^{\circ}\text{C}$ for $\text{RH} = 5\%$ (DF2) and 11% (DF3), respectively. The results show a drop in the SHG signal with respect to the signal of the mica-air interface upon freezing for the three cases DF1, DF2, and DF3. However, the relative signal drop for DF1 differs from those of DF2 and DF3. DF2 and DF3 were observed at temperatures equal to the dew points at the preset RHs, indicating two-step nucleation, first condensation, and then freezing. The coincidence of the SHG signals of the thin ice-film formed in DF2 and DF3 indicates identical structuringsimilar degree of order of water on the surface in two-step deposition freezing regardless of the onset temperature. This means that at temperatures above $-38\text{ }^{\circ}\text{C}$, growth of ice on mica apparently is a two-step process: Water first condenses and then freezes. This confirms on the molecular level the two-stage nucleation hypothesis which suggests that a nucleus forms as a liquid cluster and then freezes (Layton and Harris, 1963; Lupi et al., 2014). Further pumping of the gas mixture to the measuring cell allows for the growth of the ice-film by diffusion. The resulting ice-bulk shows a further drop in the signal for DF2 and DF3. This drop was not observed for DF1, thus indicating a major difference in the spectroscopic behavior of ice between one-step and two-step deposition freezing. To ensure that the lack of change in the SHG signal after the growth of an ice-film to ice-bulk in one-stage nucleation, DF1 figure [4a3a](#), is not an artefact, DF1 and DF2 were compared using a different system (sapphire-water interface, Fig. [4b3b](#)). Figure [4b-3b](#) shows the change in SHG intensity at the surface of sapphire for DF at -38 (black solid line and circles) and at $-23\text{ }^{\circ}\text{C}$ (red solid line and empty squares) labeled by DF1 and DF2, respectively. As in the case of mica, the drop in SHG intensity after the formation of an ice-film was followed by another drop upon further pumping of humid air of $\text{RH} = 5\%$ in the two-step freezing process (DF2), but not in one-step (DF1) freezing.



(a) Mica-ice interface



(b) Sapphire-ice interface

Figure 43: SHG intensity measured at the surfaces of mica (a) and sapphire (b) in contact with air, ice-film, and ice-bulk, respectively, collected in SM polarization combination during the three different cooling cycles, DF1: Sample cooled down first to $-38\text{ }^{\circ}\text{C}$ under dry N_2 gas, followed by pumping water vapor of $\text{RH} = 5\%$ to the measuring cell. DF2: Sample cooled down under flow of water vapor of $\text{RH} = 5\%$. DF3: Sample cooled down under flow of water vapor of $\text{RH} = 10\%$. The signal is Fresnel-corrected and normalized to the air value. All connection lines between points are just for guiding the eyes.

Figure 2-4 shows three different freezing experiments at different RHs. The gas RH was adjusted to allow liquid condensation (LC) during cooling at temperatures higher than those of deposition freezing. Constant pumping of humid air at RH = 20, 30, and 40 % and cooling down resulted in the formation of stable liquid films at -3.5, 3, and 7 °C, respectively. At all RH values, the SHG signal drops down upon the formation of a liquid-film by LC. The relative drop of the signal with respect to the air signal is similar to that observed in the DF experiments, Figure 4a3a. Comparing Figures 4a3a and 24, the SHG signals are in the same range regardless of the film phase (liquid or ice). By further pumping of humid air after LC, liquid-bulk forms at the surface with a signal that is lower than that of the liquid-film. This is mostly due to the contributions from the few secondary layers of the interfacial water. Further cooling of the sample in contact with liquid-bulk causes water to freeze by immersion freezing (IF). The observed IF temperatures for IF1, IF2, and IF3 are similar and center around $-11\text{ °C} \pm 1\text{ °C}$ which is within the range of IF temperatures observed for freezing of bulk water in contact with the surface of mica in former studies (Abdelmonem et al., 2015; Anim-Danso et al., 2016). IF produced a transient ice phase with SHG intensity higher than that of the interfacial water of the bulk liquid. The lifetime of the transient phase is around one minute, Figure 35. The values of the SHG intensities plotted in Figure 24 for transient ice-bulk are the peak values found on the transient curves shown in Figure 35 after Fresnel factor corrections and normalization to the mica-air signal. The transient phase may have had peak values higher than those obtained from Figure 35, but they were not detected due to the fast signal decay right after nucleation and the limited time resolution of signal detection of about 2.5 sec. A transient phase lasting for several minutes was reported very recently by Lovering et al. using SFG at a water-silica interface (Lovering et al., 2017). They suggested a transient existence of stacking-disordered (non-centrosymmetric) ice during the freezing process at water-mineral interfaces. Anim-Danso et al. also observed such transient ice lasting for a few tens of seconds in SFG experiments at a high-pH (9.8) solution-sapphire interface. They suggested that charge transfer and the stitching bilayer are perturbed at high pH, which leads to a decrease in SFG intensity. The present work shows that the transient ice occurs at neutral pH on mica surface and has a significant nonresonant component which is observable with the simple SHG technique. Apparently, the lifetime of the transient phase depends on the substrate and probably on the liquid-bulk size and might play a big role in the ice nucleation ability of the surface. However, this requires a comparative study involving different substrates, which will be subject of future work.

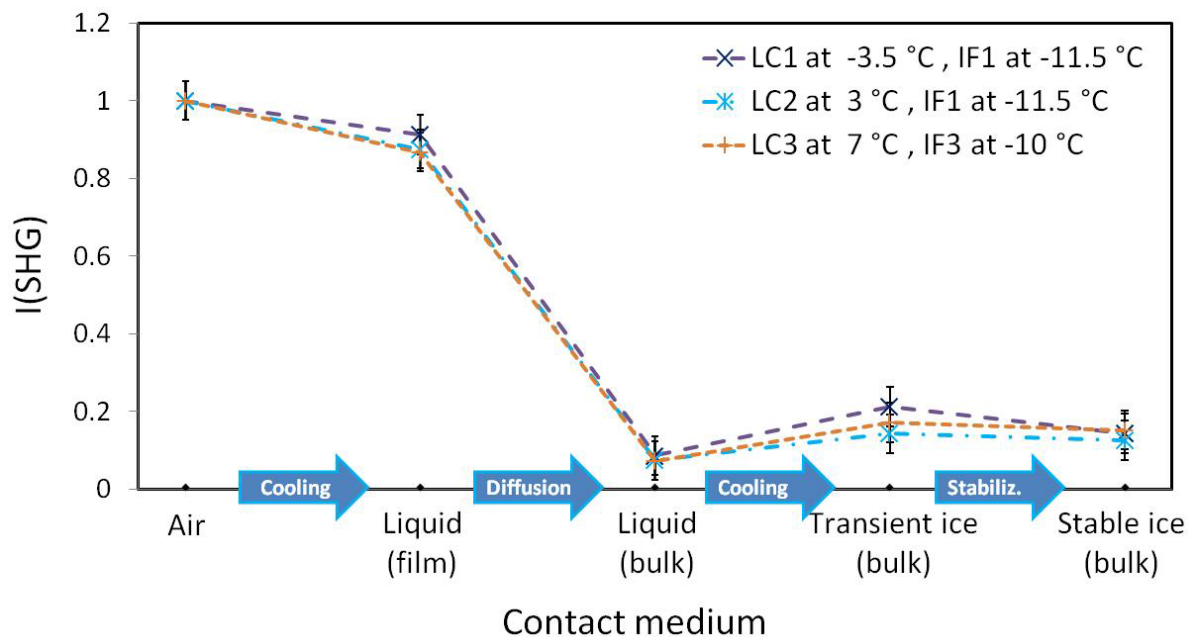


Figure 24: SHG intensity measured at the surface of mica in contact with air, liquid-film, liquid-bulk, transient ice-bulk, and stable ice-bulk, respectively, collected in SM polarization combination during three different cooling cycles, LC1 IF1: Sample cooled down under flow of water vapor of RH = 20 %. LC2 IF2: Sample cooled down under flow of water vapor of RH = 30 %.

LC3 IF3: Sample cooled down under flow of water vapor of RH = 40 % (see text for details). The signal is Fresnel-corrected and normalized to the air value. All connection lines between points are just for guiding the eyes.

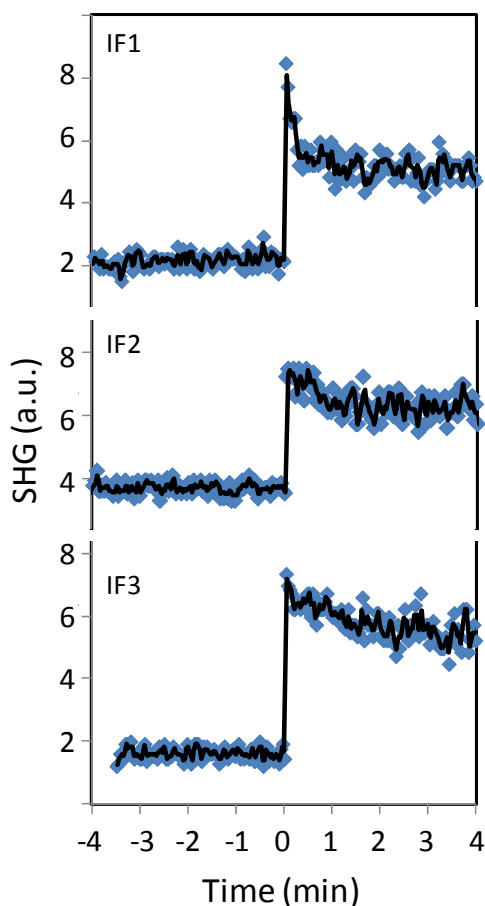


Figure 35: Typical variation in the SHG intensity around the immersion freezing points for IF1, IF2, and IF3 during the cooling experiments

Finally, I would like to comment on the drop, rather than increase, of the signal upon adsorption of water (or ice) on the surface (of either mica or sapphire). Since SHG response reflects the overall arrangements of the polar entities at the interface between two isotropic media (Fordyce et al., 2001; Goh et al., 1988; Luca et al., 1995), signal intensity is expected to increase when a single (or few non-centrosymmetric) layer(s) of water or ice is(are) formed at the surface. It is clear from Figures 43 and 24, however, that SHG intensity decreases upon deposition, freezing, condensation, and growth of liquid layers by diffusion. This can be explained by phase interference between two signals originating from two different interfacial groups of opposite dipole moments: surface-OH points out of the surface and water-OH points to the surface. A cleaved mica surface exhibits a disordered hexagonal arrangement of Si⁻ (partly Al⁻) and doubly coordinated O atoms in the outermost layer (Ostendorf et al., 2008). As an aluminosilicate mineral, this surface may protonate which hydrate immediately in contact with the ambient air (forming silanol and aluminol groups at the surface). In this case, ~~the~~ the mica-dry air signal can mainly originate from the surface hydroxyl groups (dangling-OH) which are naturally pointing out from the surface. Since mica surface is inherently negatively charged, the interfacial water-OH groups will point to the surface and thus have a phase opposite to that of the surface-OH groups, as was reported by Shen and co-workers (Zhang et al., 2008) on negatively charged surfaces. This well explains the ostensible decrease in the overall signal upon deposition and condensation. When the surface of mica is covered with bulk water of a pH ~ 7, it becomes totally deprotonated (no free-OH) ~~(Odolius et al., 1997)~~. One in four Si in the tetrahedral layers of mica is randomly substituted for Al (Christenson and Thomson, 2016). The result is that the majority of the surface hydroxyl groups of a cleaved basal plane are silanol and therefore the surface deprotonation is significantly determined by silica. The point-of-zero-charge (pzc) of silica lies between its respective isoelectric points pH 2 – 3 (Hartley et al., 1997; Iler, 1979; Scales et al., 1992) and hence the silanols in silica

(Si-OH) deprotonate totally in the presence of neutral water (pH ~ 7). Under this condition the SHG signal comes exclusively from the interfacial water molecules between the surface and liquid-bulk. This defines a new reference of the signal generated at the new interface (liquid-solid rather than gas-solid). The increase of the signal afterwards indicates more structuring of either the interfacial water before freezing, like shown in (Abdelmonem et al., 2015) or the interfacial ice after freezing like shown here. It is worth to mention that, the presence of free surface hydroxyl groups on cleaved mica is poorly discussed in literature. Miranda et al. have indirectly referred to their (hydroxyl groups) existence in their work on mica-water vapor interface using SFG (Miranda et al., 1998). They used deuterated water (D₂O) in the SFG experiments to avoid confusion of the hydroxyl stretch modes in the spectrum from both water and mica. Maslova et al. have discussed it a bit explicit in their work on surface properties of cleaved mica and they assumed that hydroxyl groups of the basal plane are not reactive (Maslova et al., 2004).

Conclusion

In summary, I used a simple SHG setup to discriminate and describe three different freezing paths on the surface of mica. The results decide on, and confirm on the molecular level, the previous speculations about the existence of two-stage deposition ice nucleation at temperatures above -38 °C. One-step and two-step deposition freezing of a thin film of ice show water structure similar to that of a thin film of liquid water. When a liquid–bulk freezes at the surface by immersion freezing, there is a transient non-centrosymmetric ice phase of high non-resonant SHG signal. The lifetime of the transient phase is suggested to be substrate–dependent and expected to affect ice nucleation efficiency. The presented results open up new horizons for the role of aerosol surfaces in promoting and stabilizing heterogeneous ice nucleation. They provide novel molecular–level insight into different ice nucleation regimes using a simple spectroscopic technique. Investigating the structuring of water molecules upon freezing next to solid surfaces is crucial to many scientific areas, such as atmospheric physics and chemistry, hydrology, and environmental and industrial applications.

The work demonstrates the worthwhile of investigating different ice nucleation processes and water structuring upon freezing on the molecular-level using SHG spectroscopy. The manuscript is considered as a cornerstone of future complementary studies involving other surfaces and other techniques to precisely investigate the layer thickness, the surface morphology effect, the cooling rates ...etc. The difficulty of characterizing monolayer films rose from the use of the IMG which required reducing the power. An alternative would be to approach the surface from the air side which then has the disadvantage of a weak SHG signal and Two-Interface Problem. These are challenges which will be tackled in future works.

Acknowledgements

The work is funded by the German Research Foundation (DFG, AB 604/1-1). The SHG setup was funded by the competence area “Earth and Environment” of KIT (start-up budget 2012). The author is grateful to Dr. A. Kiselev for his scientific discussions on ice growth and to Prof. Dr. T. Leisner, Dr. J. Lützenkirchen, Dr. C. Linke and Mrs. M. Schröder from the KIT for their support.

References

- Abdelmonem, A., Lützenkirchen, J., and Leisner, T.: Probing ice-nucleation processes on the molecular level using second harmonic generation spectroscopy, *Atmos. Meas. Tech.*, 8, 3519-3526, doi: 10.5194/amt-8-3519-2015, 2015.
- Abdelmonem, A., Backus, E. H. G., Hoffmann, N., Sánchez, M. A., Cyran, J. D., Kiselev, A., and Bonn, M.: Surface charge-induced orientation of interfacial water suppresses heterogeneous ice nucleation on α -alumina (0001), *Atmos. Chem. Phys. Discuss.*, 2017, 1-13, doi: 10.5194/acp-2017-224, 2017.
- Anim-Danso, E., Zhang, Y., and Dhinojwala, A.: Surface Charge Affects the Structure of Interfacial Ice, *J. Phys. Chem. C*, 120, 3741-3748, doi: 10.1021/acs.jpcc.5b08371, 2016.

II. Revised manuscript with tracked changes

- Balmer, T. E., Christenson, H. K., Spencer, N. D., and Heuberger, M.: The Effect of Surface Ions on Water Adsorption to Mica, *Langmuir*, 24, 1566-1569, doi: 10.1021/la702391m, 2008.
- Baron, P. A. and Willeke, K.: *Aerosol Measurement: Principles, Techniques, and Applications*, 2 ed., edited by: Sons, J., Wiley-Interscience, 2001.
- 5 Beaglehole, D., Radlinska, E. Z., Ninham, B. W., and Christenson, H. K.: Inadequacy of Lifshitz theory for thin liquid films, *Phys. Rev. Lett.*, 66, 2084-2087, 1991.
- Campbell, J. M., Meldrum, F. C., and Christenson, H. K.: Characterization of Preferred Crystal Nucleation Sites on Mica Surfaces, *Cryst. Growth Des.*, 13, 1915-1925, doi: 10.1021/cg301715n, 2013.
- 10 Campbell, J. M., Meldrum, F. C., and Christenson, H. K.: Observing the formation of ice and organic crystals in active sites, *Proceedings of the National Academy of Sciences*, 114, 810-815, doi: 10.1073/pnas.1617717114, 2017.
- Christenson, H. K. and Israelachvili, J. N.: Growth of ionic crystallites on exposed surfaces, *J. Colloid. Interface. Sci.*, 117, 576-577, doi: 10.1016/0021-9797(87)90420-6, 1987.
- Christenson, H. K. and Thomson, N. H.: The nature of the air-cleaved mica surface, *Surf. Sci. Rep.*, 71, 367-390, doi: 10.1016/j.surfrep.2016.03.001, 2016.
- 15 DeMott, P. J., Möhler, O., Stetzer, O., Vali, G., Levin, Z., Petters, M. D., Murakami, M., Leisner, T., Bundke, U., Klein, H., Kanji, Z. A., Cotton, R., Jones, H., Benz, S., Brinkmann, M., Rzesanke, D., Saathoff, H., Nicolet, M., Saito, A., Nillius, B., Bingemer, H., Abbatt, J., Ardon, K., Ganor, E., Georgakopoulos, D. G., and Saunders, C.: Resurgence in Ice Nuclei Measurement Research, *Bull. Am. Meteorol. Soc.*, 92, 1623-1635, doi: 10.1175/2011bams3119.1, 2011.
- 20 Eastwood, M. L., Cremel, S., Gehrke, C., Girard, E., and Bertram, A. K.: Ice nucleation on mineral dust particles: Onset conditions, nucleation rates and contact angles, *J. Geophys. Res.: Atmospheres*, 113, 203-201 - 203-209, doi: 10.1029/2008jd010639, 2008.
- Fordyce, A. J., Bullock, W. J., Timson, A. J., Haslam, S., Spencer-Smith, R. D., Alexander, A., and Frey, J. G.: The temperature dependence of surface second-harmonic generation from the air-water interface, *Mol. Phys.*, 99, 677-687, doi: 10.1080/00268970010030022, 2001.
- 25 Goh, M. C., Hicks, J. M., Kemnitz, K., Pinto, G. R., Heinz, T. F., Eisenthal, K. B., and Bhattacharyya, K.: Absolute orientation of water molecules at the neat water surface, *J. Phys. Chem.*, 92, 5074-5075, doi: 10.1021/j100329a003, 1988.
- Hinds, W. C.: *Aerosol Technology: Properties, Behavior, and Measurement of Airborne Particles*, 2 ed., Wiley-Interscience, 1999.
- Hoese, C. and Mohler, O.: Heterogeneous ice nucleation on atmospheric aerosols: a review of results from laboratory experiments, *Atmos. Chem. Phys.*, 12, 9817-9854, doi: 10.5194/acp-12-9817-2012, 2012.
- 30 Hu, J., Xiao, X.-D., Ogletree, D. F., and Salmeron, M.: Imaging the Condensation and Evaporation of Molecularly Thin Films of Water with Nanometer Resolution, *Science*, 268, 267-269, doi: 10.1126/science.268.5208.267, 1995.
- Jang, J. H., Lydiatt, F., Lindsay, R., and Baldelli, S.: Quantitative Orientation Analysis by Sum Frequency Generation in the Presence of Near-Resonant Background Signal: Acetonitrile on Rutile TiO₂ (110), *J. Phys. Chem. A*, 117, 6288-6302, doi: 10.1021/jp401019p, 2013.
- 35 Kiselev, A., Bachmann, F., Pedevilla, P., Cox, S. J., Michaelides, A., Gerthsen, D., and Leisner, T.: Active sites in heterogeneous ice nucleation—the example of K-rich feldspars, *Science*, doi: 10.1126/science.aai8034, 2016.
- Layton, R. G. and Harris, F. S.: Nucleation of Ice on Mica, *J. Atmos. Sci.*, 20, 142-148, doi: 10.1175/1520-0469(1963)020<0142:noiom>2.0.co;2, 1963.
- Libbrecht, K.: Growth rates of the principal facets of ice between -10°C and -40°C, *Journal of Crystal Growth*, 247, 530-540, doi: https://doi.org/10.1016/S0022-0248(02)01996-6, 2003.
- 40 Libbrecht, K. G.: The physics of snow crystals, *Rep. Prog. Phys*, 68, 855, doi: 10.1088/0034-4885/68/4/R03, 2005.
- Lovering, K. A., Bertram, A. K., and Chou, K. C.: Transient Phase of Ice Observed by Sum Frequency Generation at the Water/Mineral Interface During Freezing, *J. Phys. Chem. Lett.*, 8, 871-875, doi: 10.1021/acs.jpcclett.6b02920, 2017.
- Luca, A. A. T., Hebert, P., Brevet, P. F., and Girault, H. H.: Surface second-harmonic generation at air/solvent and solvent/solvent interfaces, *J. Chem. Soc. Faraday Trans.*, 91, 1763-1768, doi: 10.1039/ft9959101763, 1995.
- 45 Lupi, L., Kastelowitz, N., and Molinero, V.: Vapor deposition of water on graphitic surfaces: Formation of amorphous ice, bilayer ice, ice I, and liquid water, *J. Chem. Phys.*, 141, 18C508, doi: 10.1063/1.4895543, 2014.
- Mason, B. J. and Maybank, J.: Ice-nucleating properties of some natural mineral dusts, *Q. J. R. Meteorol. Soc.*, 84, 235-241, doi: 10.1002/qj.49708436104, 1958.
- Odelius, M., Bernasconi, M., and Parrinello, M.: Two Dimensional Ice Adsorbed on Mica Surface, *Phys. Rev. Lett.*, 78, 2855-2858, doi: 10.1103/PhysRevLett.78.2855, 1997.
- 50 Ong, S., Zhao, X., and Eisenthal, K. B.: Polarization of water molecules at a charged interface: second harmonic studies of the silica/water interface, *Chem. Phys. Lett.*, 191, 327-335, doi: 10.1016/0009-2614(92)85309-X, 1992.
- Ostendorf, F., Schmitz, C., Hirth, S., Kühnle, A., Kolodziej, J. J., and Reichling, M.: How flat is an air-cleaved mica surface?, *Nanotechnology*, 19, 305705, doi: 10.1088/0957-4484/19/30/305705, 2008.
- 55 Poppa, H. and Elliot, A. G.: The surface composition of Mica substrates, *Surf. Sci.*, 24, 149-163, doi: 10.1016/0039-6028(71)90225-1, 1971.
- Pruppacher, H. R. and Klett, J. D.: *Microphysics of clouds and precipitation*, 2 ed., Atmospheric and oceanographic sciences library, 18, Kluwer Academic Publishers, Dordrecht ; Boston, 954 pp., 1997.
- Rao, Y., Tao, Y.-s., and Wang, H.-f.: Quantitative analysis of orientational order in the molecular monolayer by surface second harmonic generation, *J. Chem. Phys.*, 119, 5226-5236, doi: 10.1063/1.1597195, 2003.
- 60 Schaefer, V. J.: The Formation of Ice Crystals in the Laboratory and the Atmosphere, *Chem. Rev.*, 44, 291-320, doi: 10.1021/cr60138a004, 1949.
- Shen, Y. R.: Optical Second Harmonic Generation at Interfaces, *Annu. Rev. Phys. Chem.*, 40, 327-350, doi: 10.1146/annurev.pc.40.100189.001551, 1989a.
- 65 Shen, Y. R.: Surface properties probed by second-harmonic and sum-frequency generation, *Nature*, 337, 519-525, doi: 10.1038/337519a0, 1989b.
- Slater, B., Michaelides, A., Salzmann, C. G., and Lohmann, U.: A Blue-Sky Approach to Understanding Cloud Formation, *Bull. Am. Meteorol. Soc.*, 97, 1797-1802, doi: 10.1175/bams-d-15-00131.1, 2016.
- Willeke, K. and Baron, P.: *Aerosol Measurement: Principles, Techniques, and Applications*, edited by: Klaus Willeke, P. A. B., Van Nostrand Reinhold, 1993.
- 70 Zhang, L., Tian, C., Waychunas, G. A., and Shen, Y. R.: Structures and Charging of α -Alumina (0001)/Water Interfaces Studied by Sum-Frequency Vibrational Spectroscopy, *J. Am. Chem. Soc.*, 130, 7686-7694, doi: 10.1021/ja8011116, 2008.

II. Revised manuscript with tracked changes

Zhao, X., Ong, S., and Eisenthal, K. B.: Polarization of water molecules at a charged interface. Second harmonic studies of charged monolayers at the air/water interface, *Chem. Phys. Lett.*, 202, 513-520, doi: 10.1016/0009-2614(93)90041-X, 1993.

Zhuang, X., Miranda, P. B., Kim, D., and Shen, Y. R.: Mapping molecular orientation and conformation at interfaces by surface nonlinear optics, *Phys. Rev. B*, 59, 12632-12640, doi: 10.1103/PhysRevB.59.12632, 1999.